International Journal of Environmental Sciences
ISSN: 2229-7359
Vol. 11 No. 5, 2025
https://www.theaspd.com/ijes.php

Synthesis And Characterization Of Magnetic Carbon Nanocomposites For Antimicrobial Activity And Wastewater Treatment With Microbial Fuel Cells (Mfcs)

Nalini Parashar[1], Vinod Kumar Garg[2], and Praveen Sharma[1]***
[1]Department of Environmental Science and Engineering, Guru Jambheshwar University of Science and Technology, Hisar-125001 Haryana, India
[2]Department of Environmental Sciences and Technology, Central University of Punjab, Bathinda 151001, Punjab, India
Corresponding Email: ps.enbt@gmail.com, nalini.parashar007@gmail.com

Abstract:
Wastewater treatment is critical for preserving human wellness and the ecosystem, but traditional treatment systems sometimes have limits in eliminating new pollutants while maintaining high efficiency. Over recent decades, nanotechnology has become known as a transformational tool in wastewater treatment, providing alternative options using nanomaterials. This investigation aims to synthesise and characterize magnetic carbon nanocomposites for dual implications in antimicrobial activity and remediation of pollutants from wastewater, which will be coupled with microbial fuel cells (MFCs). These nanocomposites were developed utilizing a co-precipitation process that included magnetic features with a carbonaceous matrix to improve adsorption, conductivity, and antibacterial qualities. The XRD analysis shows that the average size of the nanocomposite was 50.78 nm with a 62.43% crystalline index. In FESEM analysis, it was observed that the nanoparticles are irregular in shape with micropores and are nonuniformly arranged. For the magnetisation, VSM analysis was used and showed that the prepared nanocomposite magnetisation is 2.8 emu/g. An essential aspect of this research was the evaluation of its antibacterial activities against two distinct types of bacteria (Escherichia coli and Staphylococcus aureus). Furthermore, the role of synthesised material in the microbial fuel cell for wastewater treatment was discussed.
Keywords: *Sustainable, Magnetic Nanocomposite, Antibacterial, Wastewater Treatment, Microbial Fuel Cells.*

INTRODUCTION:

Water is essential for life, supporting food production, economic growth, and well-being [1]. Water is a controllable natural resource that can be diverted, transported, stored, and recycled efficiently [2,3]. Groundwater and surface water supplies are essential for various sectors, including agriculture, hydroelectric power generation, cattle production, forestry, fishing, navigating, and recreation [4]. Water pollution is a global environmental issue, resulting in dangerous and insufficient accessibility to purified groundwater for humans and other living species and economic growth [5-7]. Water contamination is induced by natural and manmade activity, including industrialisation and social growth, and can be catalytic [8]. Water resources contain a wide range of contaminants that are harmful to aquatic life and human health, including heavy metals, pesticides, dyes, polyaromatic hydrocarbons (PAHs), persistent organic pollutants (POPs), endocrine-disrupting compounds (EDCs), antibiotics, halocarbons, and phenols [9-12]. Approximately 12% of the world's citizens utilize contaminated and dangerous water, while almost 2.4 billion people engage in unsanitary habits that lead to environmental pollution [13]. The Asian nations, particularly Thailand, China, and Malaysia, have extensive agricultural and industrial operations that have led to water contamination in neighbouring water sources [14]. The European industry creates 90 million tons of hazardous waste [15], which might potentially pollute water bodies through its wastewater disposal. Global wastewater generation is anticipated to grow by 51% by 2050 [16]. Industries' direct release of wastewater pollutes aquatic ecosystems and groundwater, causing eutrophication and putting plant and animal health at risk [17]. Water bodies naturally purify themselves by removing contaminants through various processes [18]. The excessive sewage discharge without treatment exceeds the natural water bodies' ability to purify themselves.

Implementing the wastewater treatment process is crucial for reducing water contamination and meeting demand, particularly in regions with low incomes [19]. High-income nations have wastewater quality rules

and the required technology and resources to establish treatment facilities, whereas low-income countries lack these resources [20]. Low-income communities may face exposure to wastewater and a lack of access to clean water. Global initiatives are required to enhance the amount of effluent handled. A wide range of techniques is included in the remediation of wastewater, such as filtration, electrochemical procedures, coagulation, Fenton techniques, advanced oxidation methods, photocatalysis, and adsorptive methods [21-23]. These technologies need expensive gadgets, complex operating procedures, and extensive maintenance [24]. Some methods provide challenges when producing harmful wastes and residues [25]. Nowadays the nanotechnology provides new and extremely effective wastewater management solutions by using nanomaterials to eliminate impurities at the molecular level [26]. These nanomaterials are including nano-adsorbents, nano-catalysts, and nanomembranes, have distinct qualities such as large surface area and selective adsorption, allowing for the efficient removal of various pollutants [27]. Also, Microbial fuel cells (MFCs) are a potential wastewater treatment device that can treat wastewater while also generating power [28,29]. This dual-function solution not just decreases organic load and contaminants in wastewater, but it also generates renewable energy, making it an ecologically responsible and energy-efficient solution [30]. Further advances in MFC construction and microbiological technology are increasing its feasibility for large-scale wastewater remediation.

In this study, we aimed to synthesise magnetic activated carbon nanocomposites using a coprecipitation method for antibacterial activity and wastewater treatment with a microbial fuel cell. The structural, crystalline and morphological properties of the synthesised nanocomposite were characterised using various analytical techniques, such as Raman, XRD, FESEM with EDX. The magnetic properties of the nanocomposite were analysed using vibrating sample magnetometer techniques, and the colloidal nature and stability of the nanocomposite were analysed using zeta potential. An essential aspect of this research was the evaluation of its antibacterial activities against two distinct types of bacteria. The strain of Gram-negative Escherichia coli (E. coli) and Gram-positive Staphylococcus aureus (S. aureus) was used for antibacterial activity. Furthermore, the role of synthesised material in the microbial fuel cell for wastewater treatment was discussed.

2. MATERIALS AND METHODS

2.1 Materials

All the chemicals used in this study were of analytical grade without any mixing. Activated Charcoal AR grade, Ferrous Sulphate Heptahydrate ($FeSO_4.7H_2O$), Agar, Beef Extract, Double-distilled water and Ethanol. The solution's pH was adjusted using 0.1M NaOH solution and 0.1M HCl solution.

2.2 Synthesis of Magnetic Activated Carbon Nanocomposite

Fig. 1 depicts the schematic diagram for the synthesis method of magnetic activated carbon nanocomposite. Activated charcoal solution of 0.1 M and 0.1M ferrous sulfate heptahydrate ($FeSO_4.7H_2O$) were mixed in a 1:1 ratio and allowed to stir for 8 hours at 60 °C. The mixture was then kept undisturbed when the precipitate formed and followed by washing several times with DI water & ethanol to obtain a nanocomposite. The obtained material was then air-dried for 12 hours at 50 °C and then crushed with a motor pestle to convert it into a powder form.

Fig.1 Schematic representation of the synthesis of Magnetic Activated Carbon Nanocomposite.

2.3 Characterization of Magnetic Activated Carbon Nanocomposite

UV-visible spectroscopy of the nanocomposite was analyzed using a Varian Cary-5000 in the wavelength range of 200 to 600 nm, and Zeta potential and particle size were performed using Malvern Nano-ZS90. The X-ray diffraction (Rigaku Model) was used to analyse the crystallinity of synthesized nanocomposite at the wavelength of Cu/Ka 1.54178 Å in the range of 20-70 degrees, and the FTIR Spectrophotometer (Perkin Elmer Model) was used to record the infrared spectra. The Raman analysis was performed using Alpha300/WITec. For magnetization, a vibrating sample magnetometer was performed using Lakeshore, Model 7400. Morphology and EDX analysis were carried out using FESEM-EDAX (JEOL model).

2.4 Antimicrobial Activity:

The disc diffusion technique was used to assess the magnetic nanocomposites' antibacterial efficacy. The E. coli and S. aureus bacteria were cultivated in Luria broth (LB) with 5 g/L of beef extract, 10 g/L of peptones, 20 g/L of agar, and 5 g/L of NaCl. These had been diluted to 1×10^{-6} CFU before usage. After that, 100 µL of the indicative strain was put on the plates of nutritional agar for establishing the bacterial culture. The wells were formed by boring the agar with a sterile borer and loading 100µL using a magnetic nanocomposite with varying concentrations. These plates were incubated at 37°C for 24 hours, and the zone of inhibition could be seen.

3. RESULTS AND DISCUSSION

3.1 UV-Vis analysis of Magnetic Activated Carbon Nanocomposite

Fig. 2 depicts the optical characteristics of synthesized of magnetic activated carbon nanocomposite, which were studied using UV-VIS spectroscopy. A clear and sharp absorption peak between 300-400 nm was seen, which can be attributed to the synthesized magnetic activated carbon nanocomposite sample. A similar analysis was found by Lakshminarayanan et al., (2022) for green synthesized iron oxide nanoparticles by Bauhinia tomentosa [31].

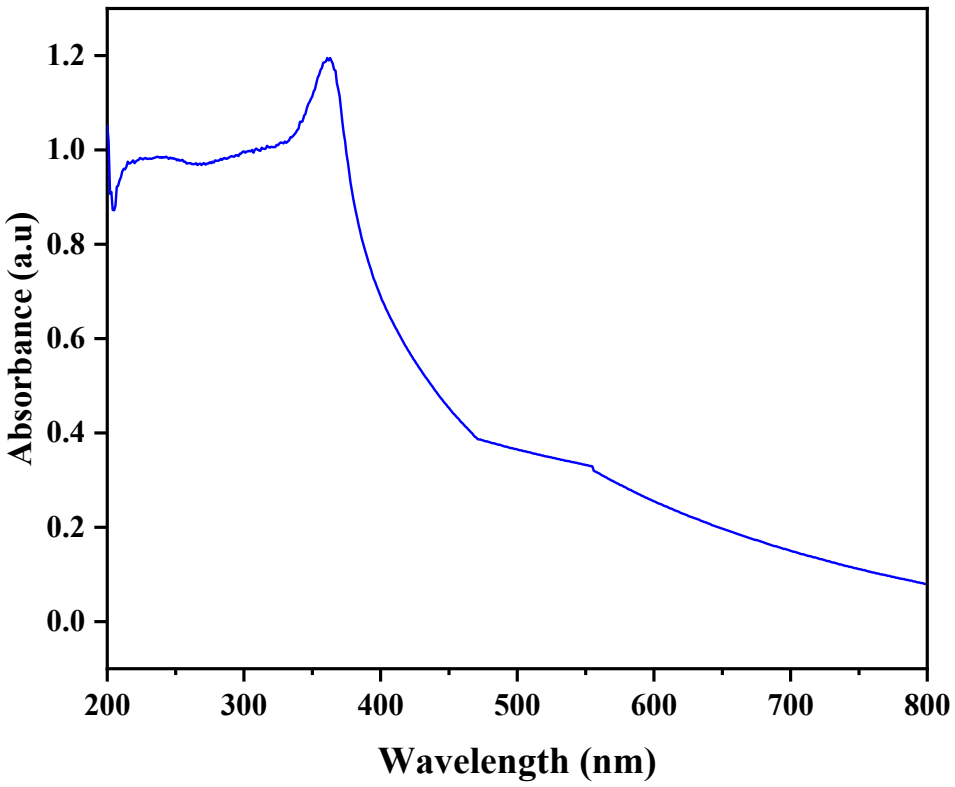

Fig. 2. UV spectrum graph of Magnetic Activated Carbon Nanocomposite.

3.2 Fourier transform infrared spectroscopy (FT-IR) analysis of Magnetic Activated Carbon Nanocomposite

The FT-IR spectrum of magnetic activated carbon nanocomposite is depicted in Fig. 3. The magnetic nanocomposite spectrum shows peaks at 490 cm^{-1} and 672 cm^{-1}, which show the stretching vibration of Fe-O bonding, and a small peak at 893 cm^{-1} shows the stretching vibration of Fe-OH bonding [32]. The two sharp peaks between 1000 cm^{-1} to 1200 cm^{-1} in the magnetic nanocomposite spectrum show the vibrational stretching of C-O bonding for the presence of alkoxy group [33]. The magnetic nanocomposite spectrum shows another peak at 1619 $cm^{-1,}$ which describes vibrational stretching of C=C bonding with sp^2 hybridisation [34]. In the nanocomposite spectrum, the wide attributed transmittance was observed at 2978 cm^{-1} to 3707 cm^{-1}, which describes the stretching of the O-H bend (Free Hydroxyl group) [35].

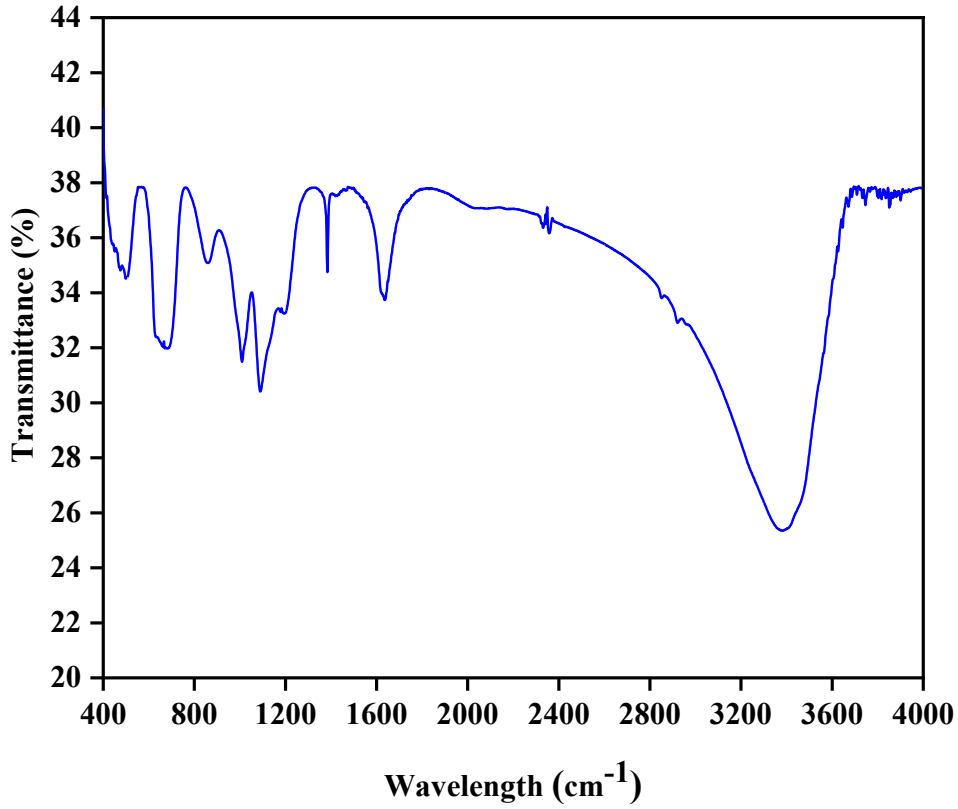

Fig. 3 FT-IR spectrum for Magnetic Activated Carbon Nanocomposite.

3.3 XRD analysis for Magnetic Activated Carbon Nanocomposite

In Fig. 4, depicted XRD analysis for magnetic activated carbon nanocomposite, where peaks corresponding to iron oxide and carbon material are clearly visible. The peaks located at 2θ angles 24.38°, 42.14°, 57.06°, and 62.18° may be assigned to the hkl values (002), (101), (511), and (440), respectively. The results match strongly with the JCPDS card no. 00–002-1357 [36]. The peaks at 2θ values 24.38° and 42.14° can be assigned to the hkl planes (002) and (101) for activated carbon material present in magnetic activated carbon nanocomposite. Further peaks at 2θ values 57.06° and 62.18° can be assigned to the hkl planes (511) and (440) for iron oxide material present in magnetic activated carbon nanocomposite. Similar results were obtained by Vitela-Rodriguez et al., (2013) when they synthesised modified iron hydroxide with activated carbon nanoparticles for arsenic removal [37]. The crystalline size of the nanocomposite was calculated using the Debye-Scherrer equation (1).

$$d = 0.9\,\lambda / \beta \cos\theta \qquad (1)$$

where d, represents the crystalline size of nanomaterial, 0.9 is a constant value as shape factor, **λ denotes the wavelength of X-ray (0.154nm), Bragg's angle in radians is denoted by θ and β refers to the FWHM (Full-Width Half Maximum) intensity of peak.**

Moreover, the average size of Magnetic Activated Carbon Nanocomposite, as obtained from the Scherrer equation, was 50.78 nm, and the crystalline index was 62.43% calculated using Equation (2).

$$\textbf{Crystalline Index}\ (\%) = \frac{\textbf{Area of Cryastalline peaks}}{\textbf{Area of all peaks}} \times \mathbf{100} \qquad (2)$$

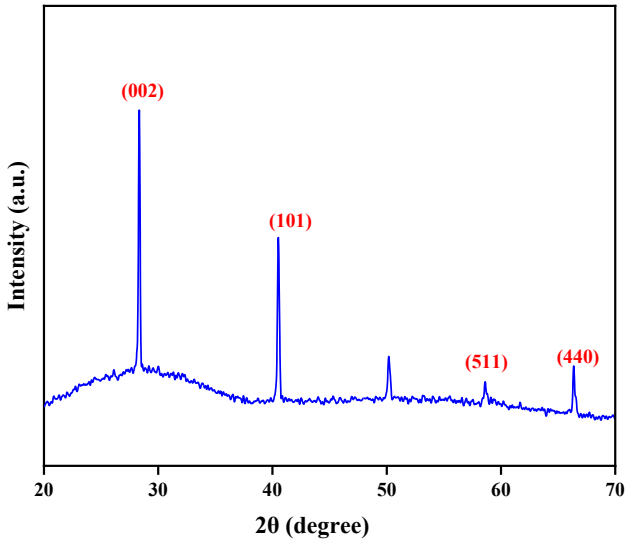

Fig. 4. XRD graph of Magnetic Activated Carbon Nanocomposite.

3.4 VSM (Vibrating Sample Magnetometer) for Magnetic Activated Carbon Nanocomposite

The VSM plot of magnetic activated carbon nanocomposite is depicted in Fig. 5, and VSM analysis was used to determine the magnetic nature of synthesized nanocomposite. It was found that the saturation magnetization (M_s) the prepared nanocomposite is 2.8 emu/g.

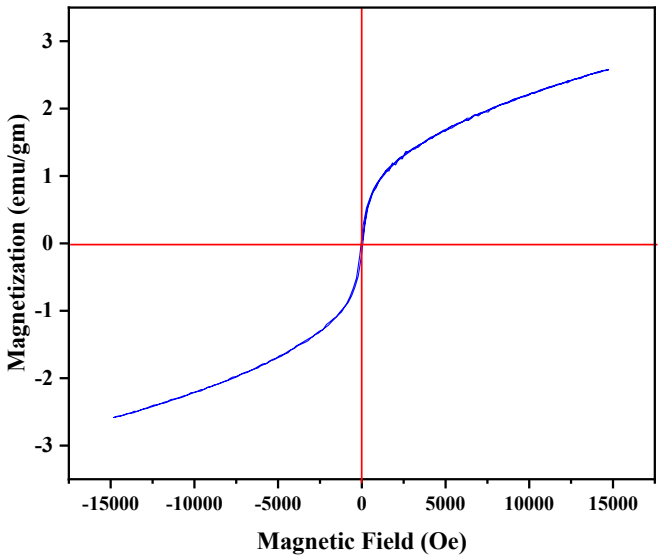

Fig. 5. VSM of Magnetic Activated Carbon Nanocomposite.

3.5 Zeta and PSA of Magnetic Activated Carbon Nanocomposite

Fig. 6 shows the zeta potential measurement of magnetic activated carbon nanocomposite with a value of -19.58 mv. The area covers 100% under the curve, indicating a homogeneous charge distribution. The negative value indicated that the nanoparticles were colloidally stable, which was crucial to avoid the accumulation of the particles and maintain the same distribution across a dispersion [38]. The DLS method allows for screening the dispersion and stability of nanoparticles in suspension based on hydrodynamic diameter. The DLS data had a sharp peak at 51 nm (Fig. 7), which confirmed that nanoparticles were also monodispersed [39]. The size of the nanocomposite is similar to the XRD data.

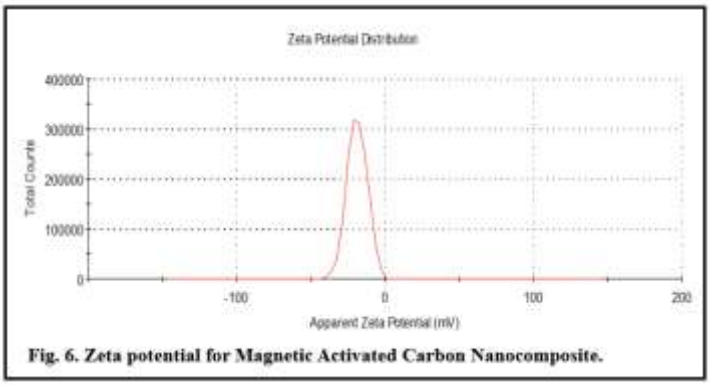

Fig. 6. Zeta potential for Magnetic Activated Carbon Nanocomposite.

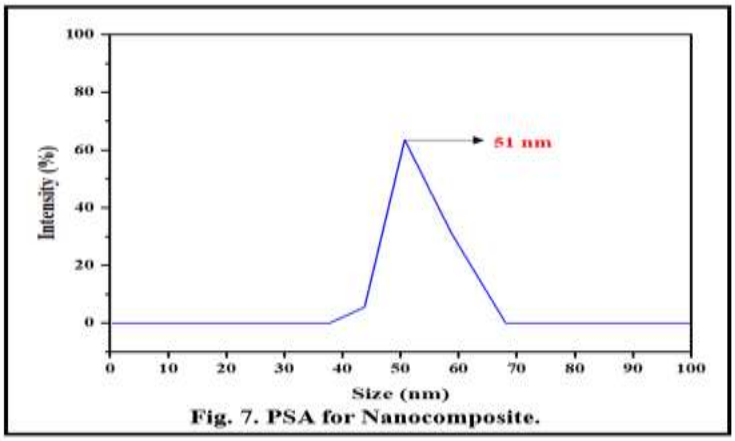

Fig. 7. PSA for Nanocomposite.

3.6 Raman analysis of Magnetic Activated Carbon Nanocomposite

The Raman spectra of magnetic activated carbon nanocomposite were shown in Fig. 8. The peaks obtained at 474 and 675 cm^{-1} can be attributed to E_g phonon modes with O-Fe-O bonding. The distinct peak appearing at 917 cm^{-1} can be attributed to the Fe-OH bond [40]. Additionally, a small peak at 1424 cm^{-1} corresponds to the carbonaceous (aromatic rings) materials prevailing in the nanocomposite.

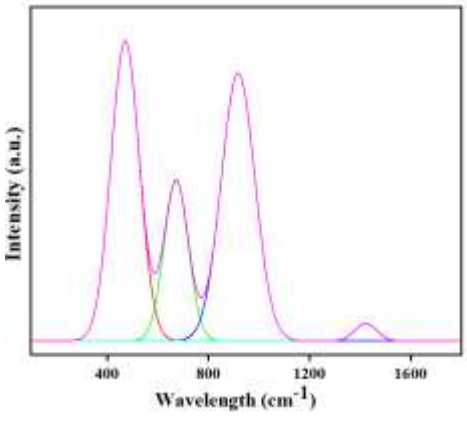

Fig. 8. Raman spectrum of Magnetic Activated Carbon Nanocomposite.

International Journal of Environmental Sciences
ISSN: 2229-7359
Vol. 11 No. 5, 2025
https://www.theaspd.com/ijes.php

3.7 FESEM analysis of Magnetic Activated Carbon Nanocomposite

In Fig. 9 depicted the FESEM analysis of magnetic activated carbon nanocomposite and it was carried out to investigate the surface morphology. From the results, it was observed that the nanoparticles are irregular in shape. However, the nanoparticles were found to be microporous, nonuniformly arranged, and some hexagonal-shaped particles can also be visible. Additionally, the nanoparticles were heterogeneous, having a mixture of smooth surface areas. Further, the EDAX image of magnetic activated carbon nanocomposite depicted in Fig. 10, which indicates the existence of activated C, Fe, and O in the sample. From EDAX analysis, it was revealed that the sample contains O is 12.7 %, Fe is 36.1 %, and 51.2 % C, which gives a clear indication of the successful formation of magnetic activated carbon nanocomposite.

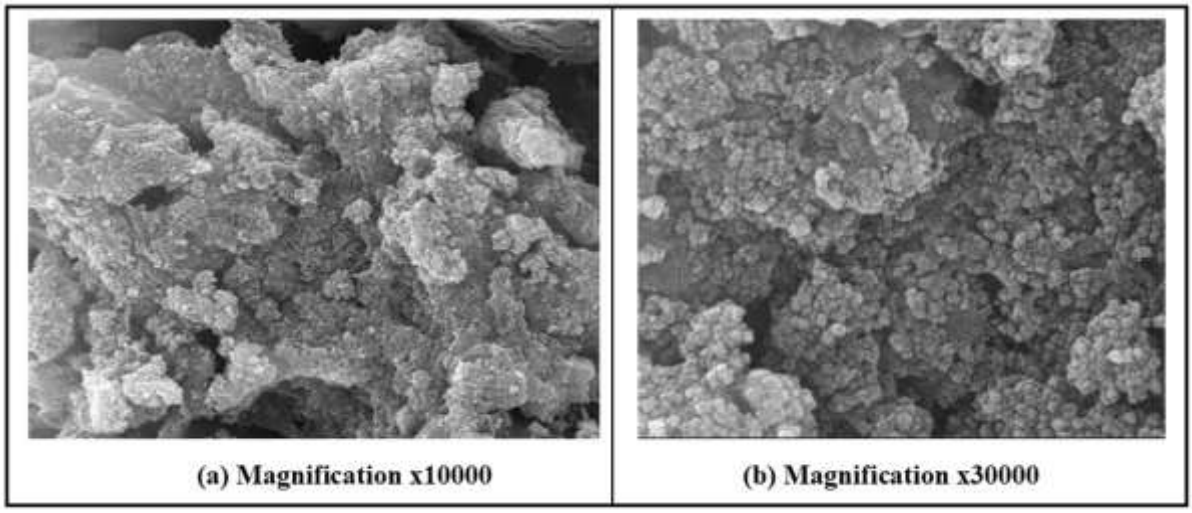

Fig. 9. FESEM images for magnetic activated carbon nanocomposite at different scales.

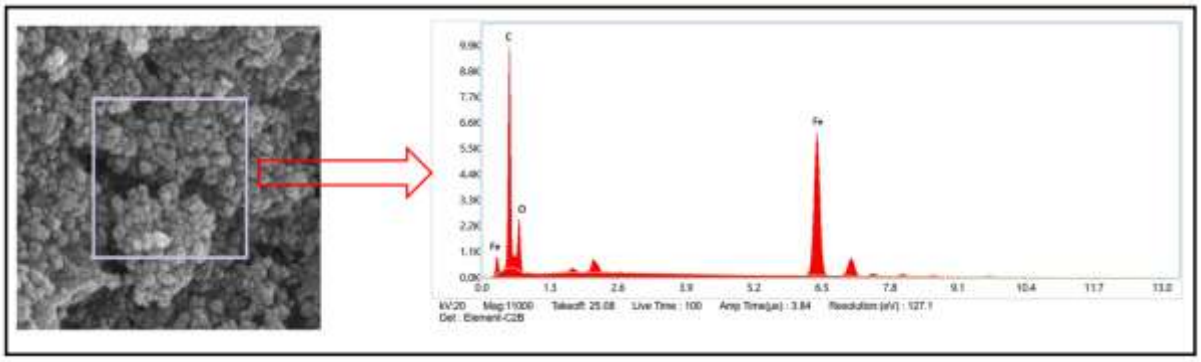

Fig. 10. EDX analysis for magnetic activated carbon nanocomposite.

3.8 Antimicrobial Activity of Magnetic Activated Carbon Nanocomposite

The antimicrobial activity of magnetic activated carbon nanocomposite with two bacteria (gram-positive and gram-negative) was successfully evaluated, which is depicted in Fig. 11. The disc diffusion method was used for bacterial strains of Staphylococcus aureus and Escherichia coli. A measurement scale was employed to calculate the diameter in millimetres for the zones of inhibition, which were the areas around the discs that impeded the growth of microbial cells. The inhibiting zones for the bacterial strain were analysed with different doses of nanocomposites have been identified and are shown in Table 1. The magnetic carbon nanocomposites tend to exhibit stronger antimicrobial activity against S. aureus compared to E. coli, because the Staphylococcus aureus has weak outer layer made with peptidoglycan layer, which is possibly more susceptible to disruption by surface interactions and oxidative stress of induced nanocomposites, but Escherichia coli possesses a tough outer membrane rich in lipopolysaccharides, which can act as a protective barrier against nanocomposite.

Table 1. Antibacterial activity parameters of Magnetic Activated Carbon Nanocomposite.

	Bacterial Strain	Inhibition Zone for Microbial Growth (mm)

Sr. No.		Control	50 µM/disc	125 µM/disc	250 µM/disc	500 µM/disc	1000 µM/disc
1.	Escherichia coli	18.5	3.5	8.2	12.7	15.3	16.1
2.	Staphylococcus aureus	21	10	12.4	15	16.9	18

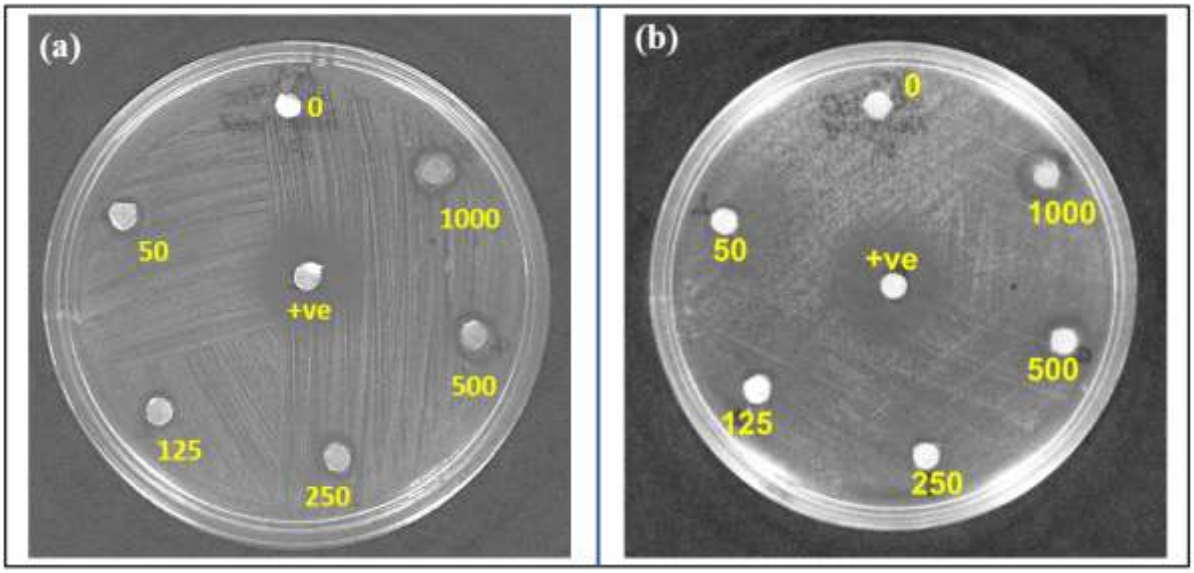

Fig. 11. Antibacterial activity on (a) Escherichia coli and (b) Staphylococcus aureus by Magnetic Activated Carbon Nanocomposite.

3.9 Magnetic Carbon Nanocomposites for Microbial Fuel Cells (MFCs)

Magnetic carbon nanocomposites have received a lot of interest for improving the performance of microbial fuel cells (MFCs) because of their unique combination of high electrical conductivity, wide surface area, and magnetic characteristics. Magnetic carbon nanocomposites, when used in microbial fuel cells (MFCs), provide an innovative and effective solution to treating wastewater by integrating superior material features with bio-electrochemical energy production. These nanocomposites act as efficient electrode materials, facilitating enhanced microbial adhesion, biofilm development, and faster electron transfer between microorganisms and the electrode surface, all of which increase power production. The magnetic characteristic also allows for better material handling and recovery, which might be useful for the MFCs device to easily maintaining and regenerating, making the treatment process more sustainable and cost-effective. Furthermore, the addition of these materials increases the breakdown of organic contaminants in wastewater while also permitting power generation.

4. CONCLUSION

In this study, successfully synthesized magnetic activated carbon nanocomposite using a coprecipitation method. The synthesized nanocomposite was analyzed by UV-vis spectroscopy, XRD, FESEM, VSM, FTIR, Zeta, and Raman analysis. All these techniques indicated the successful formation of the magnetic nanocomposite. The crystalline size of nanocomposite was 50.78 nm with a crystallinity index of 62.43%. The synthesised nanomaterial was microporous in nature. The saturation magnetization the prepared nanocomposite is 2.8 emu/g was analyzed using VSM. The zeta potential measurement of magnetic activated carbon nanocomposite with a value of -19.58 mv. According to FESEM analysis the nanocomposite is irregular shaped with nonuniformly arranged. The magnetic carbon nanocomposites tend to exhibit stronger antimicrobial activity against S. aureus compared to E. coli. Magnetic carbon nanocomposites have also received a lot of interest for improving the performance of microbial fuel cells

(MFCs) because of their unique combination of high electrical conductivity, wide surface area, and magnetic characteristics. These magnetic carbon nanocomposites are now recognized as a potential category of multipurpose materials, providing collaborative advantages in both antibacterial and wastewater treatment purposes. The nanocomposite dual functioning demonstrates their promise as sustainable and energy-effective environmental technology. Future research should concentrate on optimising composite fabrication for scaling, examining long-term environmental implications.

REFERENCES:

1. Iqbal, M. A., Akram, S., Lal, B., Hassan, S. U., Ashraf, R., Kezembayeva, G., ... & Hosseini-Bandegharaei, A. (2024). Advanced photocatalysis as a viable and sustainable wastewater treatment process: A comprehensive review. Environmental Research, 118947.
2. Zhao, Z. Y., Zuo, J., & Zillante, G. (2017). Transformation of water resource management: a case study of the South-to-North Water Diversion project. Journal of cleaner production, 163, 136-145.
3. Lane-Miller, C. C., Wheeler, S., Bjornlund, H., & Connor, J. (2013). Acquiring water for the environment: lessons from natural resources management. Journal of Environmental Policy & Planning, 15(4), 513-532.
4. Ntona, M. M., Busico, G., Mastrocicco, M., & Kazakis, N. (2022). Modeling groundwater and surface water interaction: An overview of current status and future challenges. Science of the Total Environment, 846, 157355.
5. Morin-Crini, N., Lichtfouse, E., Liu, G., Balaram, V., Ribeiro, A. R. L., Lu, Z., ... & Crini, G. (2022). Worldwide cases of water pollution by emerging contaminants: a review. Environmental Chemistry Letters, 20(4), 2311-2338.
6. Tang, W., Pei, Y., Zheng, H., Zhao, Y., Shu, L., & Zhang, H. (2022). Twenty years of China's water pollution control: Experiences and challenges. Chemosphere, 295, 133875.
7. Van Vliet, M. T., Jones, E. R., Flörke, M., Franssen, W. H., Hanasaki, N., Wada, Y., & Yearsley, J. R. (2021). Global water scarcity including surface water quality and expansions of clean water technologies. Environmental Research Letters, 16(2), 024020.
8. Singh, N., Poonia, T., Siwal, S. S., Srivastav, A. L., Sharma, H. K., & Mittal, S. K. (2022). Challenges of water contamination in urban areas. In Current directions in water scarcity research (Vol. 6, pp. 173-202). Elsevier.
9. Hojjati-Najafabadi, A., Mansoorianfar, M., Liang, T., Shahin, K., & Karimi-Maleh, H. (2022). A review on magnetic sensors for monitoring of hazardous pollutants in water resources. Science of The Total Environment, 824, 153844.
10. Singh, P. K., Kumar, U., Kumar, I., Dwivedi, A., Singh, P., Mishra, S., ... & Sharma, R. K. (2024). Critical review on toxic contaminants in surface water ecosystem: sources, monitoring, and its impact on human health. Environmental Science and Pollution Research, 31(45), 56428-56462.
11. Babuji, P., Thirumalaisamy, S., Duraisamy, K., & Periyasamy, G. (2023). Human health risks due to exposure to water pollution: a review. Water, 15(14), 2532.
12. Sharma, A., Grewal, A. S., Sharma, D., & Srivastav, A. L. (2023). Heavy metal contamination in water: consequences on human health and environment. In Metals in water (pp. 39-52). Elsevier.
13. Landrigan, P. J., Fuller, R., Acosta, N. J., Adeyi, O., Arnold, R., Baldé, A. B., ... & Zhong, M. (2018). The Lancet Commission on pollution and health. The lancet, 391(10119), 462-512.
14. Kamyab, H., Chelliapan, S., Din, M. F. M., Rezania, S., Khademi, T., & Kumar, A. (2018). Palm oil mill effluent as an environmental pollutant. Palm oil, 13(10.5772).
15. Emenike, C. U., Jayanthi, B., Agamuthu, P., & Fauziah, S. H. (2018). Biotransformation and removal of heavy metals: a review of phytoremediation and microbial remediation assessment on contaminated soil. Environmental Reviews, 26(2), 156-168.
16. Qadir, M., Drechsel, P., Jiménez Cisneros, B., Kim, Y., Pramanik, A., Mehta, P., & Olaniyan, O. (2020, February). Global and regional potential of wastewater as a water, nutrient and energy source. In Natural resources forum (Vol. 44, No. 1, pp. 40-51). Oxford, UK: Blackwell Publishing Ltd.
17. Jones, E. R., Van Vliet, M. T., Qadir, M., & Bierkens, M. F. (2021). Country-level and gridded estimates of wastewater production, collection, treatment and reuse. Earth System Science Data, 13(2), 237-254.
18. Pratiwi, D., Sumiarsa, D., Oktavia, D., & Sunardi, S. (2023). Water quality influences self-purification in the Cihawuk and Majalaya segments upstream of the Citarum river, West Java, Indonesia. Water, 15(16), 2998.
19. Owaes, M., Gani, K. M., Kumari, S., Seyam, M., & Bux, F. (2024). Implementation of partial nitrification in wastewater treatment systems by modifications in operational strategies–a review. Environmental Technology Reviews, 13(1), 379-397.
20. Singh, N., & Shreya, S. (2025). Nature-Based Solutions as Tradition in India: Lessons for Water Sustainability in the Peri-Urban. Water, 17(7), 995.
21. Sangamnere, R., Misra, T., Bherwani, H., Kapley, A., & Kumar, R. (2023). A critical review of conventional and emerging wastewater treatment technologies. Sustainable Water Resources Management, 9(2), 58.
22. Eniola, J. O., Kumar, R., Barakat, M. A., & Rashid, J. (2022). A review on conventional and advanced hybrid technologies for pharmaceutical wastewater treatment. Journal of Cleaner Production, 356, 131826.
23. Sathya, K., Nagarajan, K., Carlin Geor Malar, G., Rajalakshmi, S., & Raja Lakshmi, P. (2022). A comprehensive review on comparison among effluent treatment methods and modern methods of treatment of industrial wastewater effluent from different sources. Applied Water Science, 12(4), 70.
24. Sharma, A., & Garg, V. K. (2025). Synthesis of a novel CuO@ GO@ IR nanocomposite for the removal of tetracycline from wastewater. Environmental Science and Pollution Research, 32(2), 993-1005.

25. Garg, V. K., Kumar, N., & Anand, A. (2024). Green synthesis of nanomaterials for the removal of emerging water pollutants. In Role of Green Chemistry in Ecosystem Restoration to Achieve Environmental Sustainability (pp. 105-114). Elsevier.
26. Zhu, S., Meng, H., Gu, Z., & Zhao, Y. (2021). Research trend of nanoscience and nanotechnology–A bibliometric analysis of Nano Today. Nano Today, 39, 101233.
27. Sharma, P. K., Dorlikar, S., Rawat, P., Malik, V., Vats, N., Sharma, M., ... & Kaushik, A. K. (2021). Nanotechnology and its application: a review. Nanotechnology in cancer management, 1-33.
28. Hamedani, E. A., Abasalt, A., & Talebi, S. (2024). Application of microbial fuel cells in wastewater treatment and green energy production: a comprehensive review of technology fundamentals and challenges. Fuel, 370, 131855.
29. Feng, F., Wu, C. H., Li, F., Wang, X., Zhu, J., Zhang, R., & Chen, S. C. (2024). Research on the integration of microbial fuel cells with conventional wastewater treatment technology: Advantages of anaerobic fermentation. Energy Conversion and Management: X, 100680.
30. Hassan, M., Kanwal, S., Singh, R. S., SA, M. A., Anwar, M., & Zhao, C. (2024). Current challenges and future perspectives associated with configuration of microbial fuel cell for simultaneous energy generation and wastewater treatment. International Journal of Hydrogen Energy, 50, 323-350.
31. Lakshminarayanan, S., Shereen, M. F., Niraimathi, K. L., Brindha, P., & Arumugam, A. (2021). One-pot green synthesis of iron oxide nanoparticles from Bauhinia tomentosa: Characterization and application towards synthesis of 1, 3 diolein. Scientific Reports, 11(1), 8643.
32. Parikh, S. J., & Chorover, J. (2006). ATR-FTIR spectroscopy reveals bond formation during bacterial adhesion to iron oxide. Langmuir, 22(20), 8492-8500.
33. Brusko, V., Khannanov, A., Rakhmatullin, A., & Dimiev, A. M. (2024). Unraveling the infrared spectrum of graphene oxide. Carbon, 229, 119507.
34. 34. Morales-Cámara, S., Toral, V., Vitorica-Yrezabal, I. J., Rivadeneyra, A., Pereira, L., Rojas, S., & Romero, F. J. (2024). Simple fabrication of laser-induced graphene functionalized with a copper-based metal–organic framework and its application in solid-state supercapacitors. Journal of Materials Chemistry C, 12(21), 7784-7796.
35. 35. Ze, H., Yang, Z. L., Li, M. L., Zhang, X. G., Zheng, Q. N., Wang, Y. H., ... & Li, J. F. (2024). In situ probing the structure change and interaction of interfacial water and hydroxyl intermediates on Ni (OH) 2 surface over water splitting. Journal of the American Chemical Society, 146(18), 12538-12546.
36. Bazrafshan, A. A., Hajati, S., Ghaedi, M., & Asfaram, A. (2018). Synthesis and characterization of antibacterial chromium iron oxide nanoparticle-loaded activated carbon for ultrasound-assisted wastewater treatment. Applied Organometallic Chemistry, 32(1), e3981.
37. Vitela-Rodriguez, A. V., & Rangel-Mendez, J. R. (2013). Arsenic removal by modified activated carbons with iron hydro (oxide) nanoparticles. Journal of environmental management, 114, 225-231.
38. Yadav, D. K., Yadav, M., Mittal, R., Rani, P., Yadav, A., Bishnoi, N. R., & Singh, A. (2023). Impact of silica oxide and functionalized silica oxide nanoparticles on growth of Chlorella vulgaris and its physicochemical properties. Sustainable Chemistry for the Environment, 3, 100029.
39. Wang, D., Si, Y., Han, Y., Xie, M., Xu, L., & Sun, C. (2025). Effective activation of PMS by encapsulating monodispersed Fe3O4 within N, S heteroatoms co-doped carbon chamber for ROX removal dominated by the non-radical pathway. Separation and Purification Technology, 358, 130256.
40. Wu, J., Lin, M., Liu, M., & Chen, Z. (2024). Novel crystalline/amorphous heterophase Fe-Mn core–shell chains on-site generate hydrogen peroxide in aqueous solution. Journal of Colloid and Interface Science, 676, 227-237.